Environmental Science and Pollution Research (2021) 28:5731–5741
https://doi.org/10.1007/s11356-020-10693-4

RESEARCH ARTICLE

Application of graphene nanosheet oxide for atrazine adsorption in aqueous solution: synthesis, material characterization, and comprehension of the adsorption mechanism

Rodrigo de Souza Antônio[1] · Ana Carolina Sestito Guerra[1] · Murilo Barbosa de Andrade[1] · Letica Nishi[1] · Aline Takaoka Alves Baptista[2] · Rosângela Bergamasco[1] · Angélica Marquetotti Salcedo Vieira[3]

Received: 8 June 2020 / Accepted: 31 August 2020 / Published online: 24 September 2020

Abstract

The present study aimed to investigate the application of graphene oxide (GO) as adsorbent material for the removal of atrazine (ATZ). The material produced was characterized to investigate the characteristics and applied as an adsorbent. The material obtained after the synthesis process presented oxygenated functional groups, which contributed to the development of a good adsorbent material. Studies were carried out to verify the influence of adsorbent material mass and initial pH of ATZ solution in adsorption capacity. Kinetic study determined that pseudo-second-order model best describes adsorbate-adsorbent interaction, with equilibrium time of 72 h. The effect of temperature on the material adsorption capacity was also studied. The Langmuir isotherm is the best fit to describe adsorption process GO-ATZ and maximum adsorption capacity obtained was 23.844 ± 0.694 mg g^{-1}, at 318 K. Variations in process energies were determined, being a spontaneous adsorption, endothermic and characteristic of physical and chemical adsorption. Finally, influence of salts in solution on adsorption capacity was studied; the conclusion was that the presence of electrolytes affects the adsorption capacity of the material.

Keywords Herbicide · Emerging contaminant · Electrolytes · Removal · Graphene · Adsorption

Introduction

In recent years, several studies have reported the presence of numerous chemical compounds harmful to the environment and human health in surface and groundwater, raising concerns about the hazardous effects of these contaminants (Mijangos et al. 2018; Pinasseau et al. 2019). These chemical compounds are denominated emerging contaminants (ECs). ECs are chemical compounds of various kinds and origins, such as chemicals present in personal care products, pharmaceuticals, illicit drugs, various metabolites, and agrochemicals (herbicides, insecticides, and fungicides) (Pinasseau et al. 2019; Castiglioni et al. 2018; Mei et al. 2018).

Occurrence of ECs in water bodies is a global problem as they are aggravating the living conditions (Almeida et al. 2018; Munari et al. 2019). In addition, the ECs are still a problem in several parts of the world, such as Europe (Mijangos et al. 2018; Castiglioni et al. 2018), America (Griffero et al. 2019; Hansen et al. 2019; Sposito et al. 2018), Asia (Mei et al. 2018; Khalid et al. 2018), and Africa (Rimayi et al. 2018). Moreover, there are reports that ECs are capable of generating problems across geographical boundaries (Vystavna et al. 2018).

Due to associated risks for life and environment, herbicides are a class of ECs that are arousing alerts in the scientific community as for the presence in water bodies (Sposito et al. 2018; Sun et al. 2018). Among herbicides that are being found in surface waters, atrazine (ATZ) has been reckoned as a potential generator of environmental damage (Sposito et al. 2018; Araújo et al. 2018; Sai et al. 2018). Although this

Responsible Editor: Tito Roberto Cadaval Jr.

✉ Angélica Marquetotti Salcedo Vieira
amsvieira@uem.br

[1] Department of Chemical Engineering, State University of Maringá, 5790 - Colombo Avenue, Maringá, Parana 87020-900, Brazil

[2] Federal Technological University of Paraná, 1233, Street Rosalina Maria Ferreira, Campo Mourão, Paraná, Paraná 87301-899, Brazil

[3] Department of Food Engineering, State University of Maringá, 5790 - Colombo Avenue, Maringá, Parana 87020-900, Brazil

herbicide is banned in European Union countries, atrazine is legalized in several countries around the world, being detected in rivers in countries like Brazil (Sposito et al. 2018) and the USA (Hansen et al. 2019) as well as in drinking water in Canada (Montiel-León et al. 2019).

Because of the presence of this herbicide in water bodies, some countries regulate the maximum tolerable limit of this and other herbicides in water for human consumption, among the standards that regulate the presence of atrazine in portable water are Council Directive 98/83/EC (EU), 0.1 μg L^{-1}; Ordinance No. 5 of 2017, Annex XX, of the Ministry of Health (Brazil), 2 μg L^{-1}; and Drinking Water Standards and Health Advisories (USA), 3 μg L^{-1} (Council Directive 1998; Brasil 2017; USA 2018).

Due to the concern with the presence of ATZ in water, a risk offered by this herbicide, several studies are being developed to solve this problem, such as oxidation process (Jing et al. 2018), biosorption (Cusioli et al. 2019), catalysts (Zhang et al. 2018), cavitation with hybrid treatment (Jawale et al. 2018), and application of chemical catalysts and graphene for degradation of atrazine (Wu et al. 2018).

The adsorption technique is being extensively studied to remove emerging contaminants, as it does not generate chemical reaction by-products, it is low cost, and it is easy to implement and operate (Souza et al. 2019). There are numerous adsorbent materials that are being applied to remove herbicides from water, such as bioadsorbents (Cusioli et al. 2019), clays (Souza et al. 2019), activated carbon (Herath et al. 2019), and biochar (Herath et al. 2019; Gámiz et al. 2019). There are countless adsorbent materials being studied to remove emerging contaminants, and graphene oxide (GO) has present a promising application for removal of dyes (Wei et al. 2018), pharmaceuticals (Hiew et al. 2019), and toxic metal (Wei et al. 2018; Wang et al. 2018). The application of GO as an adsorbent material has several advantages such as chemical stability, high surface area, and availability of chemical groups on its surface (de Mendonça et al. 2018; Verma et al. 2018).

Thus, considering the presence of emerging contaminants in water bodies, an ongoing global problem, and the presence of herbicide atrazine in water bodies, still a reality in countries like Brazil and the USA, the present work has the purpose of studying the application of GO as an adsorbent material for the removal of herbicide atrazine.

Materials and methods

Synthesis of graphene oxide

Graphene oxide was synthesized according to the Hummer's method (Hummers and Offeman 1958) and modified by Kovtyukhova (1999). This process consists of oxidation of graphite using oxidizing reagents to transform graphite into graphene oxide.

Characterization of the adsorbent material

For the characterization of the synthesized adsorbent material, scanning electron microscopy coupled with energy-dispersive X-ray spectroscopy (SEM-EDX), in microscope (QUANTAFEI—250) and the sample coated with gold (Au), was used. Analyses of zeta potential (ζ) were also carried out at different pH levels with the objective of investigating charge variation present in double electrical layer of the material. The acidity or basicity was corrected with NaOH and HCl (Beckman Coulter Delsa Nano Zeta Submicron Size Analyzer™) and the structure was checked with transmission electron microscopy (TEM) (JOEL JEM—1400). X-ray diffraction analysis was performed to investigate the crystalline structure of the material (Bruker—D8 Advance), and infrared spectroscopy (Vertex70v, Bruker) was performed in order to identify functional groups present in material structure and chemical iterations formed after adsorption process.

Influence of solution pH and concentration on the adsorption capacity

The experiments were carried out in batches to investigate the influence of two factors: adsorbent concentration (mass of adsorbent/volume of ATZ solution) and initial pH of ATZ solution on adsorption capacity. The herbicide solution was prepared using distilled water and commercial atrazine supplied by Nortox S/A® (50% w/v). The studied factors were varied at three levels. The adsorbent mass was varied by 10 mg, 20 mg, and 30 mg for a solution volume of 20 mL. The solution pH was varied by 5.0 ± 0.2, 7.0 ± 0.2, and 9.0 ± 0.2. The experiments were carried out in duplicates, with a time of 24 h, temperature of 298 ± 1 K, initial concentration of atrazine solution of 10.0 mg L^{-1}, and orbital agitation of 100 rpm. After the established time, solutions were filtered using a qualitative cellulose acetate membrane with a 0.45-μm opening and permeate was read on a UV-vis spectrophotometer (Hach, DR 5000) at a wavelength of 222 nm. Adsorption capacity of the material was determined according to Eq. (1). Having determined the condition that provides the greatest adsorption capacity, kinetics and isotherm of adsorption process were performed:

$$q_i = \frac{(C_0 - C_i)V}{m_{\text{ads}}} \quad (1)$$

where q_i is the material adsorption capacity (mg g^{-1}), C_0 is the initial ATZ concentration (mg L^{-1}), C_i is the remaining ATZ concentration at given time (i) (mg L^{-1}), m_{ads} is the adsorbent mass (mg), and V is the solution volume (mL).

Kinetic study

In an established condition that provides the greatest adsorption capacity, the kinetic study was carried out. The experiment was performed in duplicate, at a constant temperature of 298 ± 1 K, initial concentration of ATZ solution of 10.0 mg L^{-1}, and GO-ATZ contact time varied from 0 to 120 h. Kinetic parameters studied were estimated according to pseudo-first-order (PFO) model (Lagergren 1898), Eq. (2):

$$q_t = q_e\left(1-e^{-k_1 t}\right) \tag{2}$$

where q_e is the material adsorption capacity at equilibrium (mg g^{-1}), and k_1 is the kinetic constant of adsorption process (h^{-1}). Another kinetic model studied was the pseudo-second order (PSO) (Blanchard et al. 1984; Ho and McKay 1999), Eq. (3):

$$q_t = \frac{q_e^2 k_2\, t}{1 + q_e k_2} \tag{3}$$

where k_2 is the kinetic constant of the adsorption process (g mg^{-1}). Then, after determining equilibrium time, the experiment for adsorption isotherm was performed.

Isotherm of adsorption

To investigate the influence of temperature on the material adsorption capacity, experiments were performed at varying initial concentration of ATZ solution from 2.0 to 30.0 mg L^{-1}, being the experimental conditions of initial pH of solution and concentration of adsorbent whose adsorption capacity presented the greatest value. As a guarantee that the system would reach the adsorption equilibrium, the established contact time was twice the time necessary for the system to reach equilibrium. Thus, isotherms at temperatures of 298 ± 1 K, 308 ± 1 K, and 318 ± 1 K were studied. Hence, to understand the influence of variation of concentration and temperature on adsorption capacity of the material, the Langmuir isotherm model was applied (Langmuir 1916), Eq. (4):

$$q_e = \frac{q_{max} K_L C_e}{1 + K_L C_e} \tag{4}$$

where q_{max} is the maximum adsorption capacity of the material at referred temperature (mg g^{-1}), K_L is the adsorption constant of the model (L mg), and Ce is the concentration of equilibrium (mg L^{-1}). Another model of isotherm studied was that of Freundlich (1906), Eq. (5):

$$q_e = K_F C_e^{\frac{1}{n}} \tag{5}$$

where K_F is the constant of Freundlich isotherm (L $g^{-1})^{1/n}$ and n is a dimensionless parameter that represents adsorbate-adsorbent interaction force.

Adsorption thermodynamics

To determine variation of thermodynamic parameters of adsorption process with the influence of temperature, Gibbs free energy (ΔG), entropy (ΔS), and enthalpy (ΔH) variations were studied. The thermodynamic relation Eq. (6) and Von't Hoff equation Eq. (7) were used to determine these parameters (Zhu et al. 2017; Tran et al. 2020):

$$\Delta G = \Delta H - T\Delta S \tag{6}$$

where ΔG is the change in Gibbs free energy (kJ mol^{-1}), ΔH the change in enthalpy (kJ mol^{-1}), T the absolute temperature of the system (K), and ΔS the entropy variation of the system (J $mol^{-1}K^{-1}$).

$$\mathrm{Ln}K_e = \frac{\Delta S}{R} - \frac{\Delta H}{RT} \tag{7}$$

where R is the thermodynamic constant (J $mol^{-1}K^{-1}$) and K_e the equilibrium constant of adsorption process determined according to the recommendations of Zhu et al. (2017).

Influence of the presence of electrolytes on the adsorption capacity

In order to investigate the influence of the presence of ions on GO adsorption capacity, parameters such as concentration and the presence of different cations can influence on GO adsorption capacity. Thus, the influence of magnesium chloride ($MgCl_2$), calcium chloride ($CaCl_2$), and sodium chloride (NaCl) salts on adsorption capacity was studied, as already studied by Zhu et al. (2017) for adsorption of metformin. For this, the same molar ratios of 0.1 mol, 0.2 mol, and 0.3 mol of salts dissolved in ATZ solution were verified. The study was carried out in duplicate, with a contact time of 24 h, a temperature of 298 ± 1 K, and initial concentration of ATZ solution of 10.0 mg L^{-1}.

Fitting data

The models were adjusted according to the Levenberg-Marquardt algorithm, with 100 iteration points, maximum limit of 400 iterations and tolerance of 10^{-9}. The criteria for determining the best fit were r^2_{adj} and χ^2. The experimental data were plotted together with respective standard deviations.

Results and discussion

Characterization of the adsorbent material

Figure 1a and b referring to the EDX analysis allow for the identification of differences in elemental composition on the

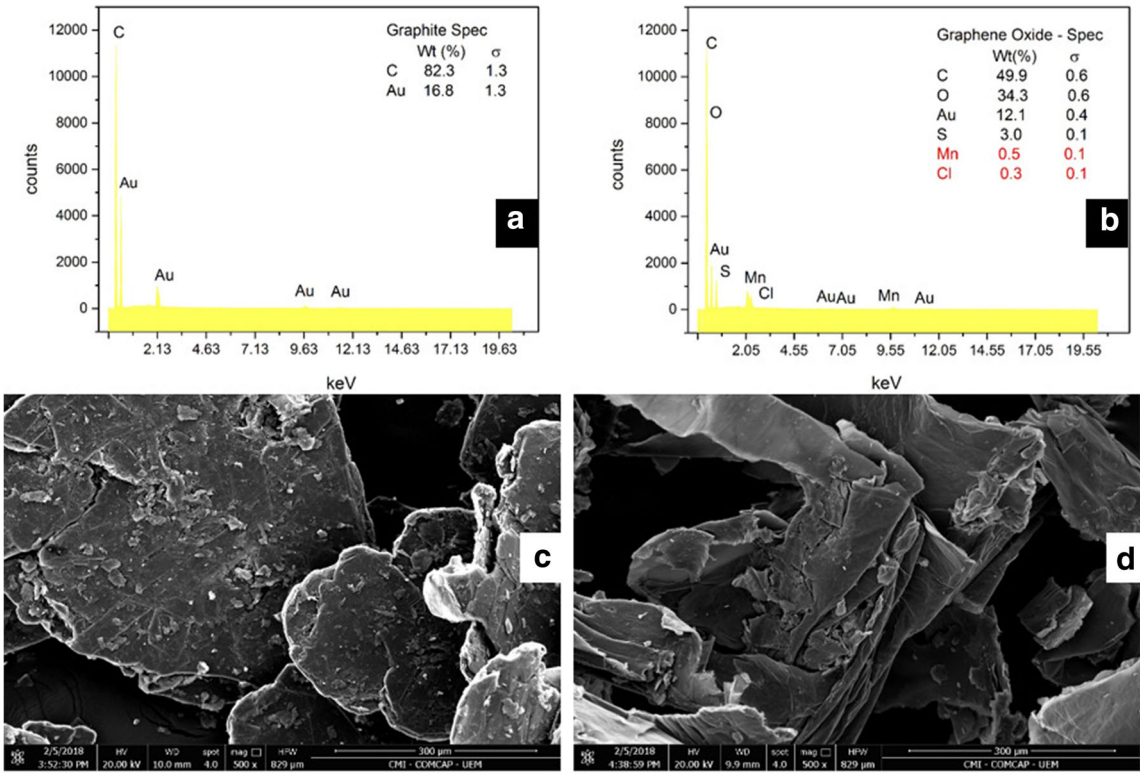

Fig. 1 EDX—graphite (**a**) and GO (**b**). SEM—× 500 magnification and 300-μm scale—graphite (**c**) and GO (**d**)

surface of graphite and graphene oxide. Graphite presents a predominantly carbon surface composition (Fig. 1a), while GO has a surface composed of chemical elements such as carbon, oxygen, sulfur, and a small amount of manganese, as shown in Fig. 1b. This finding allows us to have evidence of success of the synthesis process. When analyzing graphite surface morphology (Fig. 1c) and graphene oxide (Fig. 1d), using a scanning electron microscope, it is possible to verify differences on the surface structures of the materials.

From the XRD analysis of the materials (Fig. 2), it is possible to observe that the peak of greater intensity corresponding to graphite is obtained at 2Θ = 26.66° (002), referring to the formation structure obtained by planes of carbon atoms. For the GO obtained from graphite, the highest intensity peak occurs at 2Θ = 10.39° (001). This modification in structure is related to spacing of planes generated by insertions of oxygenated groups (Ain et al. 2018). In addition, it is possible to state that the observed change occurs due to the distance from the planes that constitute the crystalline structure of the material, since the graphite has a distance between planes equal to d = 3.38 Å, while GO is d = 8.64 Å generated by insertion of oxygenated groups, as estimated by Bragg's law (Guo et al. 2020; Kvick et al. 1999). The insertion of oxygenated groups between the GO layers after graphite oxidation can form mono-, bi-, or multilayer GO structures according to the degree of oxidation obtained during synthesis of the material, leading to separation of planes of graphite sheets and promoting changes in the material structure (de Mendonça et al. 2018).

Transmittance electron microscopy (Fig. 3) shows GO planar character and consists of few layers, giving a translucent aspect to the material. Another analysis that reinforces success of the synthesis process of the adsorbent material is the potential zeta (ζ) of GO (Fig. 4). Negative character present in double electrical layer is predominant for the entire pH range studied. This characteristic is attributed to oxygenated groups

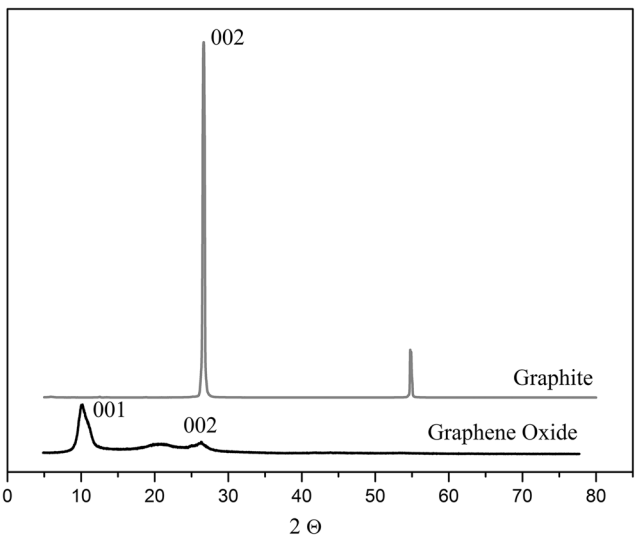

Fig. 2 XRD of graphite and graphene oxide

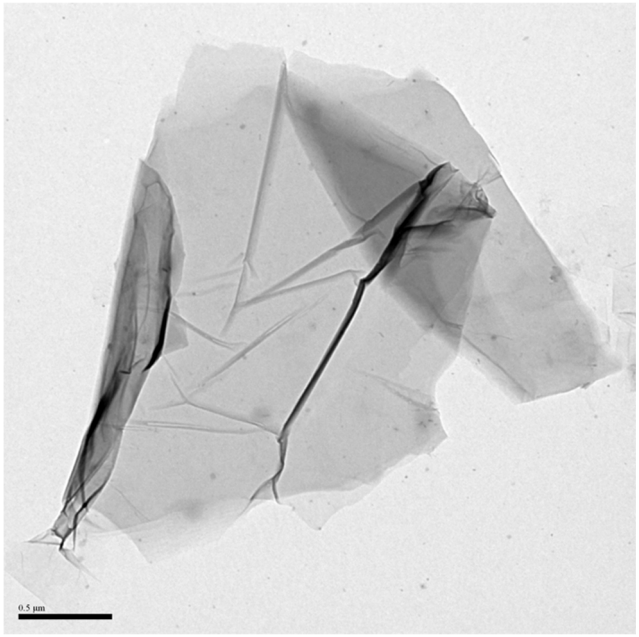

Fig. 3 TEM graphene oxide in magnification × 25 and scale of 0.5 µm

present on the surface of the material and gives a greater or lesser negative character according to the degree of oxidation obtained in the synthesis of the material (Tan et al. 2017).

Functional groups present in GO can be identified with the analysis of IR spectroscopy (Fig. 5), being possible to verify the presence of carbon/oxygen bonds existing in the material, where ~ 3668 cm^{-1} corresponds to –OH of water or hydroxyls present in the material structure. The valleys detected at ~ 1795 cm^{-1}, ~ 1653 cm^{-1}, ~ 1494 cm^{-1}, and ~ 1107 cm^{-1} correspond to the following functional groups present in GO structure: C=O corresponding to aldehyde or ketones, C=C referring to unsaturation present in carbon chain, O=CO characteristic of carboxylic groups, and C–O related to alcohol group, respectively. The last three chemical groups are being

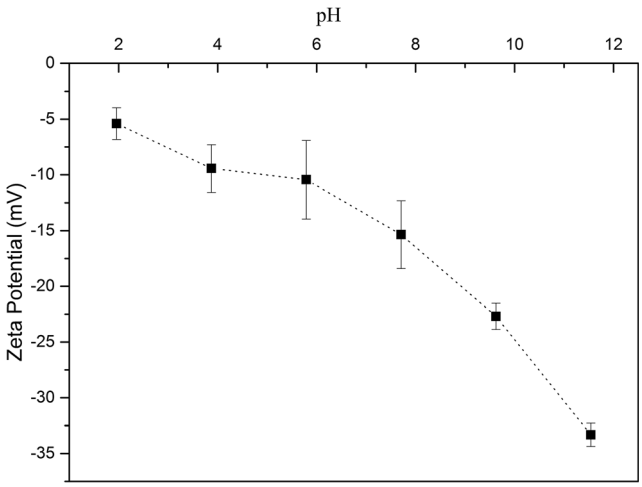

Fig. 4 Zeta potential of the GO in different pH values

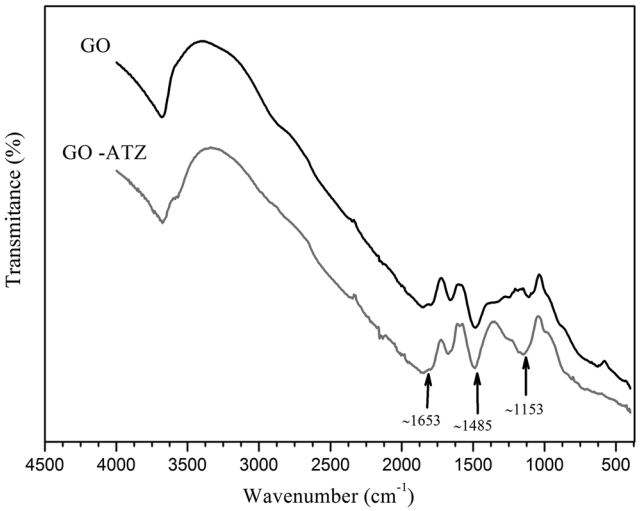

Fig. 5 IR spectrum of graphene oxide before and after adsorption process

identified as atrazine adsorption sites, as Fig. 6 suggests adsorption mechanism (Sheng et al. 2018; Lu et al. 2018).

Influence of solution pH and concentration on the adsorption capacity

Results obtained for the determination of the best adsorption conditions allow for verification that in basic initial pH, there is a favoring increase of adsorption capacity (Fig. 7). The observed value of adsorption capacity went from $q = (4.605 \pm 0.295)$ mg g^{-1}, at pH 5, to $q = (5.815 \pm 0.091)$ mg g^{-1}, at pH 9. This increase can be explained by variation of charge present in the GO electric double layer in the studied pH range, as already justified by the potential zeta (ζ) analysis.

The influence of the material adsorbent mass in the adsorption process is greater as it increases, since the remaining ATZ concentration is lower due to more availability of active sites. However, with less mass, there is an increase in the adsorption capacity which can be attributed to the diffusion mechanism acting in a limited way in the adsorption process, since the time established for the experiment was fixed at 24 h. Influence of adsorbate-adsorbent contact time was studied in kinetic study. It was possible to determine that the best condition to carry out the experiment was at initial pH of ATZ solution equal to 9 and mass of GO equal to 10 mg.

Kinetic study

Analyzing the reduction of ATZ concentration over time (Fig. 8a), it is possible to verify that after 72 h, there is no variation of ATZ concentration in aqueous phase ($dC/dt = 0$), as verified with analysis of Fig. 8b, that is, the value of the concentration became constant according to the property of the infinitesimal calculus, being possible to affirm that the system

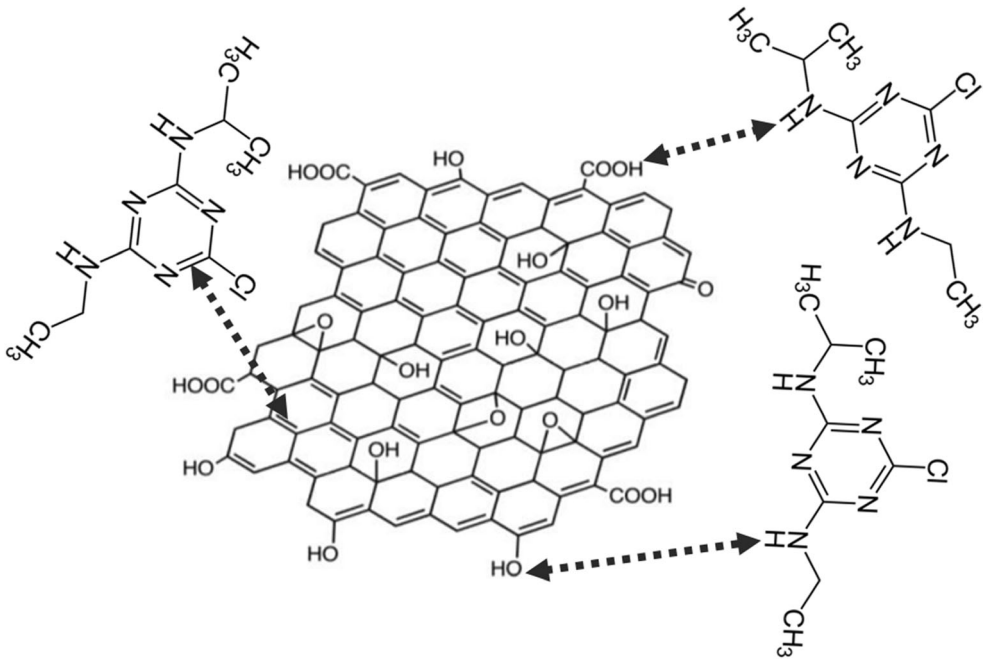

Fig. 6 Suggested atrazine adsorption mechanism in GO

reaches chemical equilibrium. From the kinetic study (Fig. 8c), it was possible to verify that the model that best represents the phenomenon of adsorption studied is the PSO model, as shown in Table 1. The justification for the PSO model presenting a better fit to studied data set is attributed to the sharp slope present at the initial period of the kinetic study. This is explained by large availability of active sites at the beginning of the adsorption process and it is reduced as ATZ is being adsorbed. Moreover, absence of adsorbate on the surface of the adsorbent material favors mass transfer mechanism, since the driving force responsible for mass transfer is the difference of concentration in the medium.

Figure 8d allows for the verification of the fidelity of the experimental data to the model that is best fitted according to

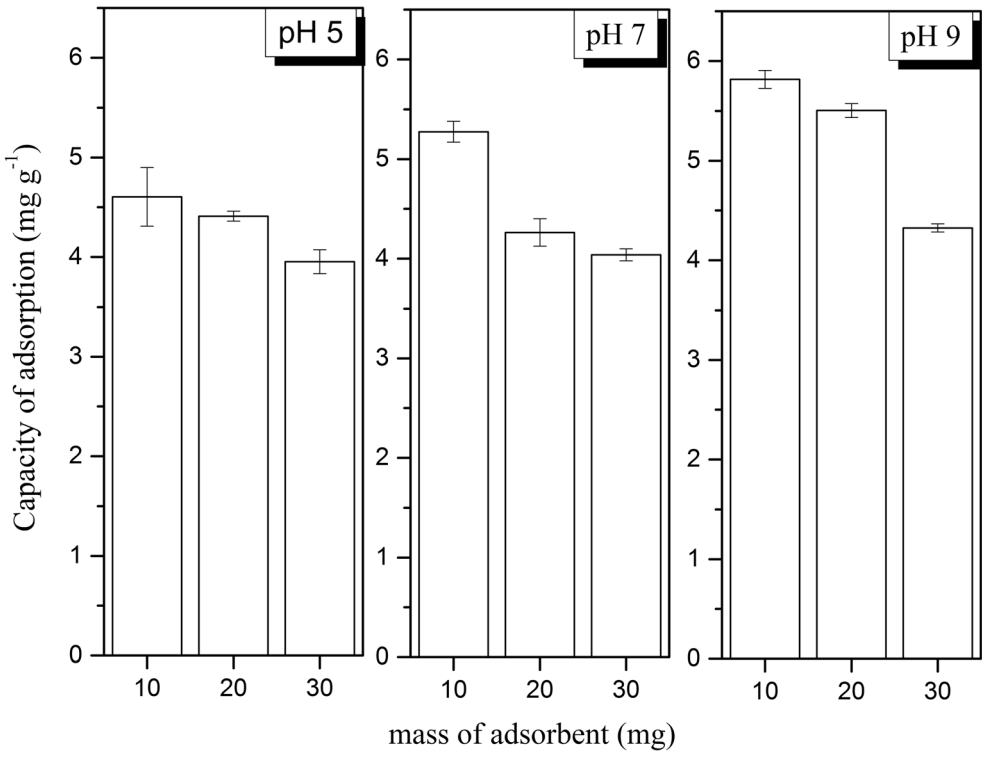

Fig. 7 Influence of adsorbent mass and pH of solution on adsorption capacity of GO

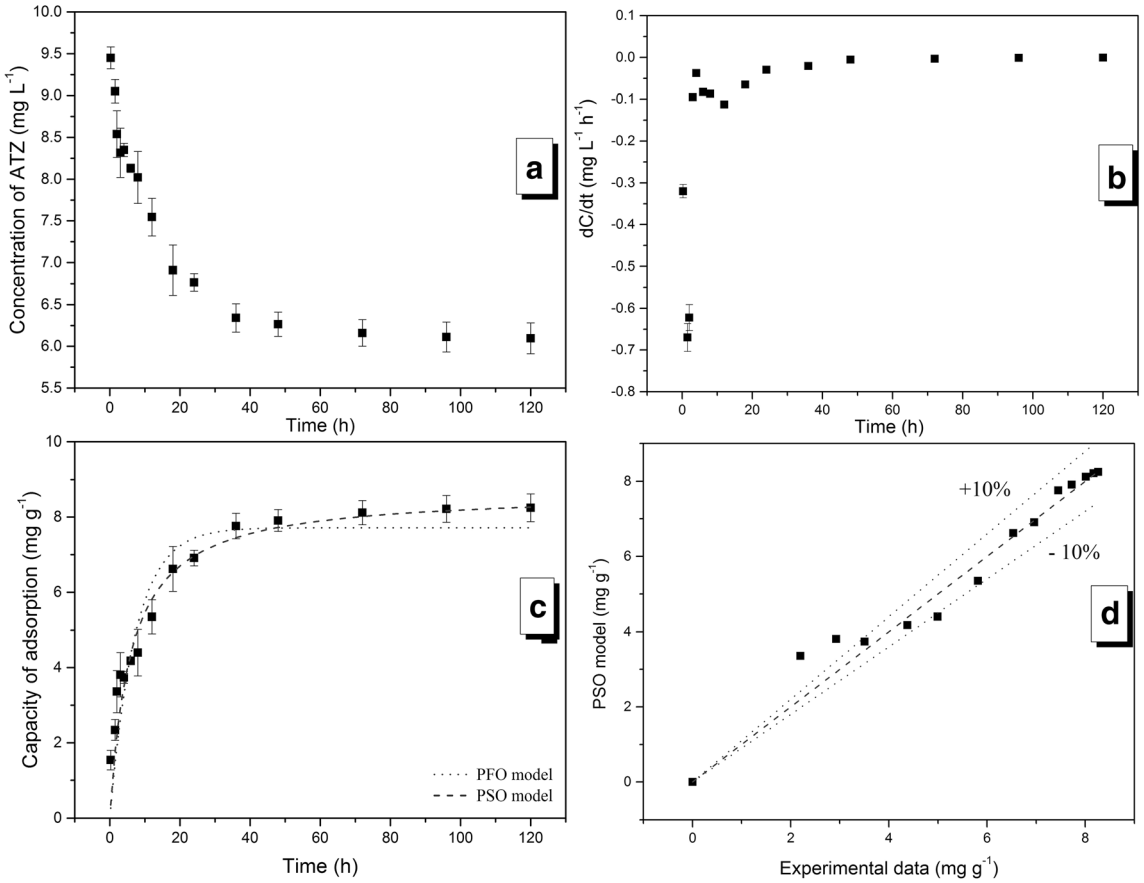

Fig. 8 Atrazine concentration reduction with time (**a**), ATZ concentration variation with time (**b**), adsorption capacity variation with time (**c**), and model validation (**d**). Experimental data (black square)

the adopted statistical criteria (r^2_{adj} and χ^2), enabling to determine if there was an error propagation during execution of experiments, as analyzed by the points on the graph bisector ($y_{PSO\ model} = x_{Experimental\ data}$). Besides this criterion, adjustments of kinetic models were analyzed according to the statistic parameters r^2_{adj} and χ^2 (Table 1).

Isotherm of adsorption

Analyzing Fig. 9 and Table 2, it is possible to state that the model that best describes the adsorption phenomenon is the Langmuir isotherm model. Isotherm model proposed by Langmuir hypothesizes that adsorption sites of material have the same adsorption energy. Such hypothesis is possible to be applied because, as already analyzed in the IR spectrum (Fig. 5) and the mechanism suggested in Fig. 6, adsorption occurs through weak chemical interactions (Van der Waals force) and

Table 1 Parameters of kinetic models studied in the present study

Model	Parameter	Value	r^2_{adj}	χ^2
PFO	k_1	0.138 ± 0.014	0.911	5.799
	q_e	7.716 ± 0.312		
PSO	k_2	0.020 ± 0.003	0.952	3.159
	q_e	8.669 ± 0.318		

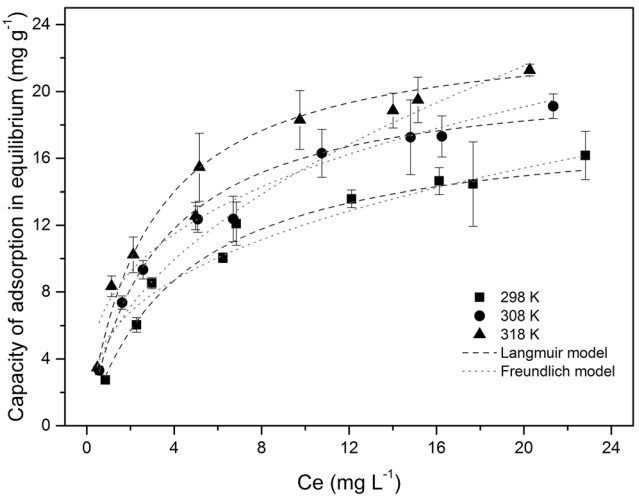

Fig. 9 Adsorption isotherms of atrazine in graphene oxide

Table 2 Parameters of isotherm models studied in this study

Langmuir model				
Temperature (K)	q_{max}(mg g^{-1})	K_L(L mg)	r^2_{adj}	χ^2
298	18.233 ± 1.363	0.228 ± 0.037	0.976	2.912
308	21.114 ± 0.656	0.317 ± 0.022	0.993	0.619
318	23.844 ± 0.694	0.356 ± 0.022	0.993	2.674
Freundlich model				
	K_F	n		
298	5.326 ± 0.124	0.355 ± 0.009	0.959	0.387
308	7.402 ± 0.172	0.316 ± 0.009	0.946	0.695
318	5.106 ± 0.226	0.480 ± 0.018	0.984	6.312

hydrogen bonds. Thus, it is possible to suggest that adsorption sites have very close adsorption energy, given hypothesis proposed by Langmuir.

In addition, analyzing Table 2, it is verified that adsorption process is favored with increase in temperature, indicating endothermic character. The maximum adsorption capacity ranges from 18.233 ± 1.363 mg g^{-1} at 298 K to 23.844 ± 0.694 mg g^{-1} at 318 K. In addition, a review in the literature showed that other authors studied different more adsorbent for removing atrazine from water, as shown in Table 3.

When buying with other works, it is possible to contact that there are different materials being developed and studied to be used as adsorbent materials, as shown in Table 3. However, a careful analysis should be made, since the Langmuir model was not always the one that best described the separation process observed by other authors. In addition, for comparison purposes, other factors should also be considered, such as adsorption conditions, physical and chemical phenomena involved, the yield of synthesis of the material, and physical characteristics of the material that may facilitate or hinder the separation process of the adsorbent material

Adsorption thermodynamics

Thermodynamic parameters obtained from Eq. (6) and Eq. (7) are shown in Table 4. It can be stated that increase in temperature makes adsorption process more spontaneous and increases, as already noted from Table 2, adsorption capacity. This increase is justified as variation in Gibbs free energy is greater as higher is the temperature ($\Delta G^{318\ K} < \Delta G^{308\ K} < \Delta G^{298\ K} < 0$). Furthermore, it was possible to quantify entropy variation, which represents the amount of energy irreversibly lost during adsorption process, being in the order of 108.415 J $mol^{-1}K^{-1}$. Enthalpy is the energy available through the adsorption system; the value of ΔH found states that the adsorption process is endothermic, that is, the heat flow occurs from the environment to the adsorption system. The magnitude of variation of the enthalpy suggests that GO-ATZ has characteristically physical adsorption interactions with indications of the presence of stronger chemical bonds, such as hydrogen bonds, detected in the IR spectrum.

Table 3 Maximum adsorption capacity obtained by the Langmuir isotherm at 298 K by different authors

Absorbent		q_{max} (mg g^{-1}) of the Langmuir isotherm	References
Magnetic multi-walled carbon nanotube		40.16	Tang et al. 2012
Moringa oleifera Lam.		0.653	Coldebella et al. 2018
Seed Shell Activated Carbon		3.235	Giwa et al. 2018
Metal-organic framework	Type: ZIF-8	6.78	Akpinar and Yazaydin 2018
	Type: UiO-66	2.57	
	Type: UiO-67	10.96	
Modified *Moringa oleifera* Lam. seed husks		4.297	Cusioli et al. 2019
Graphene oxide impregnated with iron oxide		38.814	Andrade et al. 2019
Graphene Oxide		18.233	This work

Table 4 Thermodynamic parameters of adsorption process

Temperature (K)	ΔG (kJ mol^{-1})	ΔH (kJ mol^{-1})	ΔS (J mol^{-1}K^{-1})
298	− 2.766	+ 29.480	+ 108.415
308	− 4.404		
318	− 4.926		

Influence of the presence of electrolytes on the adsorption capacity

The influence of the presence of electrolytes in solution on adsorption capacity can be observed in Fig. 10. The presence of sodium chloride (NaCl), calcium chloride ($CaCl_2$), and magnesium chloride ($MgCl_2$) salts in the same molar ratio is unfavorable to the adsorption process, as there was a reduction in adsorption capacity when compared with solution without the presence of ions.

It is possible to verify that salts in which cations are bivalent (Ca^{2+} and Mg^{2+}); there is a greater reduction in adsorption capacity than salt whose cation is monovalent (Na^{+}). The explanation is that the amount of dissociated ions in the system is different when comparing monovalent salt $\left(YCl_{(s)} \rightarrow Y^{+}_{(aq)} + Cl^{-}_{(aq)}\right)$ with divalent salts $\left(XCl_{2(s)} \rightarrow X^{2+}_{(aq)} + 2Cl^{-}_{(aq)}\right)$. Furthermore, it was also possible to verify that adsorption capacity was reduced with increase in molarity of salts, and similar results were obtained by Tan et al. (2017) and Zhu et al. (2017).

Conclusion

In this study, it is possible to conclude that graphene oxide (GO) can be used as an adsorbent material for removal of atrazine herbicide. The chosen chemical synthesis process gives GO functional groups on its surface that is an excellent site for adsorption. Thus, adsorbent material chosen showed favorable characteristics for the adsorption of herbicide, as it was possible to verify with suggested adsorption mechanisms and maximum adsorption capacity determined. It was found that the most appropriate kinetic model to describe the process is the pseudo-second order. In addition, it is possible to affirm that there is an influence of temperature on adsorption capacity in equilibrium and that maximum adsorption capacity is favored with the increase of temperature. The maximum adsorption capacity varied from 18.233 ± 1.363 mg g^{-1}at temperature of 298 K to 23.844 ± 0.694 mg g^{-1} at 318 K. Regarding adsorption thermodynamics, the process is considered thermodynamically favorable since variation in Gibbs free energy (ΔG) is negative. Heat exchanged during adsorption process is of an endothermic nature with an order of magnitude characteristic of physical adsorption promoted by $\pi - \pi$ bonds together with hydrogen bonds. Finally, it was also possible to observe that the presence of electrolytes favors adsorption process as concentration of salts increases and according to characteristic of cation present in salt.

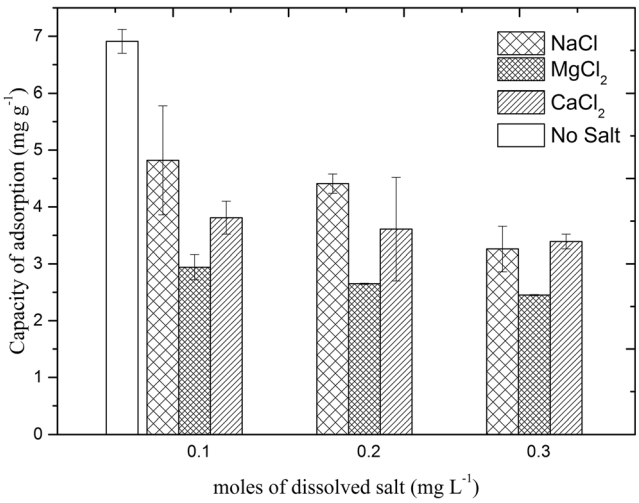

Fig. 10 Influence of the presence of salts on adsorption capacity of the material

Acknowledgments The authors thank the Higher Education Personnel Improvement Coordination (CAPES, Financing Code 001), National Council for Scientific and Technological Development (CNPq), the Complex of Research Support Centers (COMCAP), and Chemical Engineering Department (DEQ) of the State University of Maringá (UEM).

References

Ain QT, Al-Modlej A, Alshammari A, Anjum MN (2018) Effect of solvents on optical band gap of silicon-doped graphene oxide. Mater Res Express 5. https://doi.org/10.1088/2053-1591/aab239

Akpinar I, Yazaydin AO (2018) Adsorption of atrazine from water in metal-organic framework materials. J Chem Eng Data 63:2368–2375. https://doi.org/10.1021/acs.jced.7b00930

Almeida MD, Pereira TSB, Batlouni SR, Boscolo CNP, Almeida EA (2018) Estrogenic and anti-androgenic effects of the herbicide tebuthiuron in male Nile tilapia (Oreochromis niloticus). Aquat Toxicol 194:86–93. https://doi.org/10.1016/j.aquatox.2017.11.006

Andrade MB, Santos TRT, Fernandes Silva M, Vieira MF, Bergamasco R, Hamoudi S (2019) Graphene oxide impregnated with iron oxide nanoparticles for the removal of atrazine from the aqueous medium. Sep Sci Technol 54:2653–2670. https://doi.org/10.1080/01496395.2018.1549077

Araújo CVM, Silva DCVR, Gomes LET, Acayaba RD, Montagner CC, Moreira-Santos M, Ribeiro R, Pompêo MLM (2018) Habitat fragmentation caused by contaminants: atrazine as a chemical barrier isolating fish populations. Chemosphere 193:24–31. https://doi.org/10.1016/j.chemosphere.2017.11.014

Blanchard G, Maunaye M, Martin G (1984) Removal of heavy metals from waters by means of natural zeolites. Water Res 18:1501–1507. https://doi.org/10.1016/0043-1354(84)90124-6

Brasil (2017) Portaria de Consolidação nº 5, de 28 de Setembro de 2017

Castiglioni S, Davoli E, Riva F, Palmiotto M, Camporini P, Manenti A, Zuccato E (2018) Mass balance of emerging contaminants in the

water cycle of a highly urbanized and industrialized area of Italy. Water Res 131:287–298. https://doi.org/10.1016/j.watres.2017.12.047

Coldebella PF, Fagundes-Klen MR, Rezende D, Alves Baptista AT, Nishi L, Shimabuku QL, Bergamasco R (2018) Ecofriendly biosorption of atrazine herbicide in aqueous solution by moringa oleifera lam: kinetics, equilibrium and thermodynamics. Desalin Water Treat 126:248–258. https://doi.org/10.5004/dwt.2018.22907

Council Directive (1998) 98/83/Ec. Off J Eur Communities L330:32–54

Cusioli LF, Bezerra C d O, Quesada HB, Baptista ATA, Nishi L, Vieira MF, Bergamasco R (2019) Modified Moringa oleifera Lam. Seed husks as low-cost biosorbent for atrazine removal. Environ Technol 14:1–12. https://doi.org/10.1080/09593330.2019.1653381

de Mendonça JPA, Lima AH, Roldao JC, Martins J d S, Junqueira GMA, Quirino WG, Sato F (2018) The role of sulfate in the chemical synthesis of graphene oxide. Mater Chem Phys 215:203–210. https://doi.org/10.1016/j.matchemphys.2018.05.022

Freundlich HMF (1906) Uber die Adsorption in Losungen, Zeitschrift Für Phys. Chemie 57:385–470

Gámiz B, Hall K, Spokas KA, Cox L (2019) Understanding activation effects on low-temperature biochar for optimization of herbicide sorption. Agronomy 9:588. https://doi.org/10.3390/agronomy9100588

Giwa SO, Moses JS, Adeyi AA, Giwa A (2018) Adsorption of atrazine from aqueous solution using desert date seed shell activated carbon. ABUAD J Eng Res Dev 1:317–325

Griffero L, Alcántara-Durán J, Alonso C, Rodríguez-Gallego L, Moreno-González D, García-Reyes JF, Molina-Díaz A, Pérez-Parada A (2019) Basin-scale monitoring and risk assessment of emerging contaminants in South American Atlantic coastal lagoons. Sci Total Environ 697:134058. https://doi.org/10.1016/j.scitotenv.2019.134058

Guo R, Li H, Liu H (2020) Phase investigation and crystal structure analysis of zinc stannate (Zn2SnO4). Phys Lett A 384:10. https://doi.org/10.1016/j.physleta.2019.126205

Hansen SP, Messer TL, Mittelstet AR (2019) Mitigating the risk of atrazine exposure: identifying hot spots and hot times in surface waters across Nebraska, USA. J Environ Manag 250:109424. https://doi.org/10.1016/j.jenvman.2019.109424

Herath GAD, Poh LS, Ng WJ (2019) Statistical optimization of glyphosate adsorption by biochar and activated carbon with response surface methodology. Chemosphere. 227:533–540. https://doi.org/10.1016/j.chemosphere.2019.04.078

Hiew BYZ, Lee LY, Lee XJ, Gan S, Thangalazhy-Gopakumar S, Lim SS, Pan GT, Yang TCK (2019) Adsorptive removal of diclofenac by graphene oxide: optimization, equilibrium, kinetic and thermodynamic studies. J Taiwan Inst Chem Eng 98:150–162. https://doi.org/10.1016/j.jtice.2018.07.034

Ho YS, McKay G (1999) Pseudo-second order model for sorption processes. Process Biochem 34:451–465. https://doi.org/10.1016/S0032-9592(98)00112-5

Hummers WS, Offeman RE (1958) Preparation of graphitic oxide. J Am Chem Soc 80:1339. https://doi.org/10.1021/ja01539a017

Jawale RH, Dapurkar O, Gogate PR (2018) Treatment of atrazine containing wastewater using cavitation based hybrid treatment approaches. Chem Eng Process – Process Intensif 130:275–283. https://doi.org/10.1016/j.cep.2018.06.017

Jing L, Chen B, Wen D, Zheng J, Zhang B (2018) The removal of COD and NH3-N from atrazine production wastewater treatment using UV/O3: experimental investigation and kinetic modeling. Environ Sci Pollut Res 25:2691–2701. https://doi.org/10.1007/s11356-017-0701-z

Khalid NK, Devadasan D, Aravind UK, Aravindakumar CT (2018) Screening and quantification of emerging contaminants in Periyar River, Kerala (India) by using high-resolution mass spectrometry (LC-Q-ToF-MS). Environ Monit Assess 190(6):370. https://doi.org/10.1007/s10661-018-6745-9

Kovtyukhova NI (1999) Layer-by-layer assembly of ultrathin composite films from micron-sized graphite oxide sheets and polycations. Chem Mater 11:771–778. https://doi.org/10.1021/cm981085u

Kvick Å, Synchrotron E, Facility R (1999) Mass transport studied using NMR spectroscopy materials science applications of X-ray. (1999), 1248–1257.

Lagergren S (1898) Zur theorie der sogenannten adsorption gelster stoffe, Kungliga Svenska Vetenskapsakademiens. Handlingar 24:1–34

Langmuir I (1916) The constitution and fundamental properties of solids and liquids. Part I. Solids. J Am Chem Soc 38:2221–2295. https://doi.org/10.1021/ja02268a002

Lu L, Wang J, Chen B (2018) Adsorption and desorption of phthalic acid esters on graphene oxide and reduced graphene oxide as affected by humic acid. Environ Pollut 232:505–513. https://doi.org/10.1016/j.envpol.2017.09.078

Mei X, Sui Q, Lyu S, Wang D, Zhao W (2018) Pharmaceuticals and personal care products in the urban river across the megacity Shanghai: occurrence, source apportionment and a snapshot of influence of rainfall. J Hazard Mater 359:429–436. https://doi.org/10.1016/j.jhazmat.2018.07.081

Mijangos L, Ziarrusta H, Ros O, Kortazar L, Fernández LA, Olivares M, Zuloaga O, Prieto A, Etxebarria N (2018) Occurrence of emerging pollutants in estuaries of the Basque Country: analysis of sources and distribution, and assessment of the environmental risk. Water Res 147:152–163. https://doi.org/10.1016/j.watres.2018.09.033

Montiel-León JM, Duy SV, Munoz G, Bouchard MF, Amyot M, Sauvé S (2019) Quality survey and spatiotemporal variations of atrazine and desethylatrazine in drinking water in Quebec, Canada. Sci Total Environ 671:578–585. https://doi.org/10.1016/j.scitotenv.2019.03.228

Munari M, Matozzo V, Chemello G, Riedl V, Pastore P, Badocco D, Marina MG (2019) Seawater acidification and emerging contaminants: A dangerous marriage for haemocytes of marine bivalves. Environ Res 175:11–21. https://doi.org/10.1016/j.envres.2019.04.032

Pinasseau L, Wiest L, Fildier A, Volatier L, Fones GR, Mills GA, Mermillod-Blondin F, Vulliet E (2019) Use of passive sampling and high resolution mass spectrometry using a suspect screening approach to characterise emerging pollutants in contaminated groundwater and runoff. Sci Total Environ 672:253–263. https://doi.org/10.1016/j.scitotenv.2019.03.489

Rimayi C, Odusanya D, Weiss JM, de Boer J, Chimuka L (2018) Science of the Total Environment Contaminants of emerging concern in the Hartbeespoort Dam catchment and the uMngeni River estuary 2016 pollution incident , South Africa. Sci Total Environ 627:1008–1017. https://doi.org/10.1016/j.scitotenv.2018.01.263

Sai L, Li L, Hu C, Qu B, Guo Q, Jia Q, Zhang Y, Bo C, Li X, Shao H, Ng JC, Peng C (2018) Identification of circular RNAs and their alterations involved in developing male Xenopus laevis chronically exposed to atrazine. Chemosphere 200:295–301. https://doi.org/10.1016/j.chemosphere.2018.02.140

Sheng G, Huang C, Chen G, Sheng J, Ren X, Hu B, Ma J, Wang X, Huang Y, Alsaedi A, Hayat T (2018) Adsorption and co-adsorption of graphene oxide and Ni(II) on iron oxides: A spectroscopic and microscopic investigation. Environ Pollut 233:125–131. https://doi.org/10.1016/j.envpol.2017.10.047

Souza FM, dos Santos OAA, Vieira MGA (2019) Adsorption of herbicide 2,4-D from aqueous solution using organo-modified bentonite clay. Environ Sci Pollut Res 26:18329–18342. https://doi.org/10.1007/s11356-019-05196-w

Sposito JCV, Montagner CC, Casado M, Navarro-Martín L, Jut Solórzano JC, Piña B, Grisolia AB (2018) Emerging contaminants in Brazilian rivers: occurrence and effects on gene expression in

zebrafish (Danio rerio) embryos. Chemosphere 209:696–704. https://doi.org/10.1016/j.chemosphere.2018.06.046

Sun S, Chen Y, Lin Y, An D (2018) Science of the Total Environment Occurrence , spatial distribution , and seasonal variation of emerging trace organic pollutants in source water for Shanghai, China. Sci Total Environ 639:1–7. https://doi.org/10.1016/j.scitotenv.2018.05.089

Tan P, Bi Q, Hu Y, Fang Z, Chen Y, Cheng J (2017) Effect of the degree of oxidation and defects of graphene oxide on adsorption of Cu 2+ from aqueous solution. Appl Surf Sci 423:1141–1151. https://doi.org/10.1016/j.apsusc.2017.06.304

Tang WW, Zeng GM, Gong JL, Liu Y, Wang XY, Liu YY, Liu ZF, Chen L, Zhang XR, Tu DZ (2012) Simultaneous adsorption of atrazine and Cu (II) from wastewater by magnetic multi-walled carbon nanotube. Chem Eng J 211–212:470–478. https://doi.org/10.1016/j.cej.2012.09.102

Tran HV, Hoang LT, Huynh CD (2020) An investigation on kinetic and thermodynamic parameters of methylene blue adsorption onto graphenebased nanocomposite. Chem Phys 535:110793. https://doi.org/10.1016/j.chemphys.2020.110793

USA U- (2018) 2018 edition of the drinking water standards and health advisories Tables

Verma A, Parashar A (2018) Molecular dynamics based simulations to study the fracture strength of monolayer graphene oxide. Nanotechnology 29. https://doi.org/10.1088/1361-6528/aaa8bb

Vystavna Y, Frkova Z, Celle-Jeanton H, Diadin D, Huneau F, Steinmann M, Crini N, Loup C (2018) Science of the Total Environment Priority substances and emerging pollutants in urban rivers in Ukraine : Occurrence , fl uxes and loading to transboundary European Union watersheds. Sci Total Environ 637–638:1358–1362. https://doi.org/10.1016/j.scitotenv.2018.05.095

Wang X, Liu Y, Pang H, Yu S, Ai Y, Ma X, Song G, Hayat T, Alsaedi A, Wang X (2018) Effect of graphene oxide surface modification on the elimination of Co(II) from aqueous solutions. Chem Eng J 344:380–390. https://doi.org/10.1016/j.cej.2018.03.107

Wei M-P, Chai H, Cao Y-L, Jia D-Z (2018) Sulfonated graphene oxide as an adsorbent for removal of Pb2+ and methylene blue. J Colloid Interface Sci 524:297–305. https://doi.org/10.1016/j.jcis.2018.03.094

Wu S, Li H, Li X, He H, Yang C (2018) Performances and mechanisms of efficient degradation of atrazine using peroxymonosulfate and ferrate as oxidants. Chem Eng J 353:533–541. https://doi.org/10.1016/j.cej.2018.06.133

Zhang H, Liu X, Ma J, Lin C, Qi C, Li X, Zhou Z, Fan G (2018) Activation of peroxymonosulfate using drinking water treatment residuals for the degradation of atrazine. J Hazard Mater 344:1220–1228. https://doi.org/10.1016/j.jhazmat.2017.11.038

Zhu S, Liu YG, Liu SB et al (2017) Adsorption of emerging contaminant metformin using graphene oxide. Chemosphere 179:20–28. https://doi.org/10.1016/j.chemosphere.2017.03.071